Hydrol. Earth Syst. Sci. Discuss., 4, 2273–2306, 2007
www.hydrol-earth-syst-sci-discuss.net/4/2273/2007/

Hydrology and Earth System Sciences Discussions

Papers published in *Hydrology and Earth System Sciences Discussions* are under open-access review for the journal *Hydrology and Earth System Sciences*

Comparison of soil moisture fields estimated by catchment modelling and remote sensing: a case study in South Africa

T. Vischel[1,*], G. Pegram[1], S. Sinclair[1], W. Wagner[2], and A. Bartsch[2]

[1]Civil Engineering Programme, University of KwaZulu-Natal, Durban 4041, South Africa
[2]Institute of Photogrammetry and Remote Sensing, Vienna University of Technology, Austria
[*]now at: Laboratoire d'étude des Transferts en Hydrologie et Environnement (UMR 5564), 38000 Grenoble, France

Received: 28 June 2007 – Accepted: 4 July 2007 – Published: 12 July 2007

Correspondence to: T. Vischel (theo.vischel@hmg.inpg.fr)

Abstract

The paper compares two independent approaches to estimate soil moisture at the regional scale over a 4625 km^2 catchment (Liebenbergsvlei, South Africa). The first estimate is derived from a physically-based hydrological model (TOPKAPI). The second estimate is derived from the scatterometer on board on the European Remote Sensing satellite (ERS). Results show a very good correspondence between the modelled and remotely sensed soil moisture, illustrated over two selected seasons of 8 months by regression R^2 coefficients lying between 0.78 and 0.92. Such a close similarity between these two different, independent approaches is very promising for (i) remote sensing in general (ii) the use of hydrological models to back-calculate and disaggregate the satellite soil moisture estimate and (iii) for hydrological models to assimilate the remotely sensed soil moisture.

1 Introduction

The content of water in the first active metres of soil plays a central role in the regulation of the hydraulic and energy transfers between the soil, the surface and the atmosphere. Soil moisture is thus widely recognized as a key variable in numerous environmental disciplines especially in meteorology, hydrology and agriculture. For hydrological and agricultural purposes, the estimation of soil moisture is crucial since it controls (i) the quantity of water available for the growth of vegetation (Rodriguez-Iturbe, 2000), as well as the recharge of deep aquifers (Hodnett and Bell, 1986); (ii) the saturation of soils which controls the partitioning of rainfall between runoff and infiltration (Merz and Plate, 1997). In meteorology, the soil moisture content has a great impact on the transfer of energy from the surface into the atmosphere since it controls the evapotranspiration fluxes (Entekhabi et al., 1996).

An accurate estimation of soil moisture is difficult to obtain since it is highly variable in both space and time (Western and Blöschl, 1999). The two main sources of soil mois-

ture information come from ground-based and remote sensing estimations. In the field, data can be obtained from gravimetric sampling, this gives the most accurate measurement of the soil water content but is obviously not suitable for automation. Probes (Neutron or Time Domain Reflectometry) can be easily calibrated to also provide an accurate and possibly automated estimation of soil moisture. Ground observations have helped to document soil moisture patterns at plot to hillslope scales (less than 1 km^2) in different regions of the world (e.g. Grayson et al., 1997; McNamara et al., 2005; De Lannoy et al., 2006; Hébrard et al., 2006). However, when catchment scales are of interest, one is rapidly confronted with scaling issues (Western and Blöschl., 1999) since ground measurements provide soil moisture estimation limited (i) to small spatial support (from few centimetres for probes, to 1 m for gravimetric sampling) and (ii) to relatively small areas (extension in the order of a few hectares) since the implementation of a probe network of large extent is subject to obvious logistical and economic constraints.

Remote sensing of soil moisture from satellites is a promising alternative to ground measurements. Microwave frequencies are most often used, both in active (scatterometer or SAR) and passive (radiometer) instruments, to estimate soil moisture (see Wagner et al., 2007 for a detailed review). The advantage of microwave remote sensing is that it provides extended soil moisture estimations, gridded on averaged surface (footprint) from tens of metres to 50 km resolution, scales more suitable for catchment hydrology. However microwave estimations are only representative of the top few centimeters of soil, provided that the vegetation is not too dense, and the data availability is often dependent on a low frequency repeat cycle at a point (from 1 day to several weeks depending on the satellite).

Due to the uncertainties associated with the estimation of soil moisture, Kostov and Jackson (1993) suggest that the ideal approach for estimating soil moisture is to combine soil moisture measurements with hydrological models by using assimilation techniques. In fact, remotely sensed soil moisture is often directly assimilated into hydrological models (Ottlé and Vidal-Madjar,1994; Pauwels et al., 2002; Aubert et al., 2003;

Parajka et al., 2006) or into land surface schemes (Bruckler and Witono, 1989; Houser et al., 1998; Reichle et al., 2001; Walker et al., 2001) in order to initialize, drive, update and/or re-calibrate models, with the main objective of improving the simulations of river discharges or atmospheric fluxes respectively. However, very few studies in the literature compare the estimations of soil moisture from remote sensing with the estimations from hydrological models (Biftu and Gang, 2001; Parajka et al., 2006). One must however be able to know a priori the compatibility between the model and remotely sensed soil moisture estimations to better evaluate the effective potential of (i) hydrological models to provide back-calculated estimations of soil moisture for evaluating remotely sensed soil moisture, followed by the use of physical disaggregation tools to improve the low resolution typical of remotely sensed soil moisture fields, (ii) remotely sensed soil moisture estimates to be assimilated into hydrological models. Wagner et al. (2003) point out the necessity of comparing remotely sensed soil moisture with independent data derived from ground observations, models and/or other remote sensing techniques. Blyth (2002) mentions the necessity of modelling the soil moisture in detail and intercomparing models and data. Pellenq et al. (2003) argue that it is essential to accurately understand all the processes involved in the soil moisture variability and their scale interactions. For that purpose, Western et al. (2002) point out the potential of process-based hydrological models that explicitly represent the dynamic and the spatial scales of the processes that control the soil moisture.

In the present study, we compare two independent approaches of soil moisture estimation on a regional size catchment in South Africa (Liebenbergsvlei, 4625 km^2). The first estimations are derived from the physically-based distributed hydrological model TOPKAPI (Liu and Todini, 2002). The second estimations are derived from the scatterometer on board on the European Remote Sensing satellite ERS.

The region, data and hydrological model are presented in Sect. 2. In Sect. 3, the capacity of the TOPKAPI model to mimic the discharges on the studied catchment is evaluated. In Sect. 4, the modelled and remotely sensed soil moisture estimates are compared. The results are discussed in Sect. 5.

2 Region, data and hydrological model

2.1 Characteristics of the Liebenbergsvlei catchment

The Liebenbergsvlei catchment (4625 km^2) is located in the Free State province of South Africa (Fig. 1). The climate is semi-arid, characterized by a mean annual rainfall between 600 and 700 mm and a mean annual evapotranspiration between 1400 and 1500 mm. The landscape is characterized by (i) hillslopes and steep relief in the southern part of the catchment which corresponds to the border of the Lesotho and the Maluti mountains, (ii) grassland and cropland over the bulk of the catchment since farming is the main activity in the region. These features are shown in the two first digital maps of Fig. 2a (Digital Elevation Model-DLSI, 1996; and Landcover/use-GLCC, 1997). Information about soil properties is also available (Fig. 2a, Soil type-SIRI, 1987; Soil texture-Midgley et al., 1994).

2.2 Hydrologic data set

Rainfall and flow data

Hydrological data are available on the catchment (Fig. 3). A unique rain gauge network consisting of 45 tipping bucket rain gauges provided 5 min. time step ground rainfall measurement for the period 1993–2002.

Two flow gauges (labelled 1 and 2 in Fig. 3) are available at the outlet of the catchment and further upstream, with unequal data availability and quality between 1993 and 2001. External flows arrive from Lesotho via an inter-basin transfer, beginning in September 1997. These inter-basin transfer flows are recorded at a station located at the outlet of the transfer tunnel (labelled 3 in Fig. 3). The quality of the flow data stations 1 and 2 has improved since 2002, but the recent flow data are not considered since the dense rain gauge network was no longer operational after the year 2002.

Satellite derived soil moisture data

The remotely sensed soil moisture estimates used in this study are derived from scatterometers on-board of the satellites ERS-1 and ERS-2 (Wagner et al., 2003). The ERS scatterometer is a C-band radar (5.3 GHz), operational since 1991 up to at least 2007, which has acquired data with a spatial resolution of 50 km with a vertical polarization at a 25 km grid spacing. Global coverage is achieved by the satellite every 3 or 4 days on average, but since the ERS scatterometer is in operational conflict with the ERS Synthetic Aperture Radar, only a part of the coverage is effectively available for scatterometer measurements. The repeat cycle at one point is thus 7 days on average, varying irregularly from 3 to 10 days. ERS scatterometer grid points over the Liebenbergvlei are represented by the red crosses on Fig. 3. Over Southern Africa, ERS data are available until 2000.

Scatterometer microwave radiation data are very sensitive to the moisture content of the surface soil layer due to the strong variation of the dielectric constant of the soil with water content. However other factors influence the scatterometer backscatter signal. Retrieval soil moisture methods must mainly take into account the effects of vegetation, surface roughness and heterogeneous land cover. The retrieval method technique adopted for the data used here is based on the change detection method proposed by Wagner et al. (1999a). To account for effects of roughness and heterogeneous land cover, the lowest and highest values of backscatter coefficients are determined (respectively σ^0_{dry} and σ^0_{wet}) on the nine-year measurement period 1992–2000. The two limiting reference values are assumed to be representative of the vegetated land surface under respectively dry and saturated soil conditions. The measured backscatter coefficients are then compared to σ^0_{dry} and σ^0_{wet}, resulting in the definition of topsoil moisture contents m_s (<5 cm) interpreted as a relative quantity ranging between 0 and 1 (respectively, 0–100%), scaled between zero soil moisture and saturation. At any

time t, m_s is then defined as:

$$m_s(t) = \frac{\sigma^0(t) - \sigma^0_{\text{dry}}}{\sigma^0_{\text{wet}} - \sigma^0_{\text{dry}}} \quad (1)$$

The effects of plant growth and decay are taken into account through the application of varying seasonally σ^0_{dry} and σ^0_{wet} values as proposed by Wagner et al. (1999b). This method exploits the multi-incidence capabilities of the ERS scatterometer to describe the effect of enhanced volume scattering in the vegetation layer and the corresponding decrease of the ground scattering contribution.

2.3 The hydrological model TOPKAPI

TOPKAPI is an acronym which stands for TOPographic Kinematic APproximation and Integration and is a physically-based distributed rainfall-runoff model. In the original version proposed by Liu and Todini (2002), TOPKAPI consists of five main modules comprising soil, overland, channel, evapotranspiration and snow modules. The first three are modules in the form of non-linear reservoirs controlling the horizontal flows. The reservoir equations are approximated by the kinematic wave model differential equations at a point. The well-known point-scale differential equations are then analytically integrated in space to the finite dimension of a grid cell, which is taken to be a pixel of the digital elevation model (DEM) that describes the topography of the catchment. The evapotranspiration module implemented for this study has been slightly modified compared to the original module presented in Liu and Todini (2002). The snow module component is ignored in the present study as the influence of snow can be neglected for the Liebenbergsvlei catchment.

Model assumptions

The TOPKAPI model is based on six fundamental assumptions (Liu and Todini, 2002):

1. Precipitation is constant in space and time over the integration domain (namely the single grid cell or pixel and the basic time interval, usually few hours).
2. All precipitation falling on the soil infiltrates, unless the soil is already saturated (Dunne, 1978).
3. The slope of the groundwater table coincides with the slope of the ground.
4. Local transmissivity, like horizontal subsurface flow in a cell, depends on the integral of the total water content of the soil in the vertical.
5. In the soil surface layer, the saturated hydraulic conductivity is constant with depth and, due to macro-porosity, is much larger than in deeper layers.
6. During the transition phase, the variation of water content in time is constant in space.

Ordinary Differential Equations controlling the reservoir flows

The equations of each of the three reservoirs (soil, overland and channel) that compose a cell i can be written as a classical differential equation of continuity:

$$\frac{dV_i}{dt} = Q_i^{\text{in}} - Q_i^{\text{out}} \tag{2}$$

where all the variables are observed at time t: V_i is the total volume stored in the reservoir, $\frac{dV_i}{dt}$ is the rate of change of water storage, Q_i^{in} is the total inflow rate to the reservoir, $Q_i^{\text{out}}$is the total outflow rate from the reservoir.

The kinematic wave approach used to resolve the continuity and mass balance in TOPKAPI (by neglecting the dynamic acceleration terms in the energy equation) leads to a nonlinear relationship between Q_i^{out} and V_i, turning Eq. (2) into to an ordinary differential equation (ODE) of the form:

$$\frac{dV_i}{dt} = Q_i^{\text{in}} - b_i V_i^{\alpha} \tag{3}$$

where b_i is constant in time (it frequently varies spatially) and is a function of the geometrical and physical characteristics of the reservoir. b_i also depends on the exponent coefficient α which originates from either the infiltration equations describing soil reservoir behaviour or from Manning's equations used in the overland and channel reservoir specifications (see Liu and Todini, 2002 for more details about the theoretical basis). For the three reservoirs (soil, overland and channel), the expressions of b_i and α are reported in Table 1. Depending on the type of reservoir, Q_i^{in} is a combination of the forcing variables (interconnecting flows between the elemental storage reservoirs within the cell and from upper connected cells and including rainfall and evapotranspiration in the case of the soil reservoir; Table 2).

At each simulation time step, the inflow rate Q_i^{in} is computed, assumed to be a constant over the interval, then the ODE equation is solved by numerical integration. In this application of TOPKAPI a combination of a quasi–analytical solution (proposed by Liu and Todini, 2002) with a numerical integration procedure based on the Runge-Kutta-Fehlberg method was used (Gerald and Wheatley, 1992). This fast, numerically stable and accurate hybrid scheme was used to integrate the appropriate variations of Eq. (3) over the time interval Δt, dependent on the initial volume stored in the reservoir at time t, to obtain the volume $V_i(t+\Delta t)$ stored at $t+\Delta t$. This solution of Eq. (3) differs from the method recommended by Liu and Todini (2002) and was chosen after carefully examining the ability of the various solutions to numerically satisfy the continuity equations at each time step and in each cell. In Table 2 all the variables that are computed for each reservoir from the ODE finite difference solution showing the reservoir and cell connectivity are reported. Table 2 is associated with Fig. 4 which illustrates the fluxes and connections for a typical modelled cell.

Evapotranspiration

The evapotranspiration module was slightly modified from the original version of Liu and Todini (2002). In the channel, the evaporation is extracted at the rate of the potential evaporation of a free surface of water. On the hillslopes, the actual evapotran-

spiration is computed as a proportional ratio of the reference crop evapotranspiration depending on a constant crop factor k_c and the current saturation of the reservoir computed at each time step.

3 Comparison between modelled and observed discharges

3.1 Modelling features

Selected period

From the data set presented in Sect. 2.2, two seasons of eight months were selected during which the rainfall and flow data were both continuous and of good quality. The first season (Season 1) between November 1993 and June 1994 was used to adjust the parameters of the TOPKAPI model. The second season (Season 2) between November 1999 and June 2000 is used in Sect. 3.2 as a model verification period. In both seasons the modelled soil moisture is compared with the corresponding remotely sensed soil moisture in Sect. 4.

Model resolution

The model spatial resolution was imposed by the desire to use a freely available DEM at 1 km (DLSI, 1996; see Sect. 2.1). A 6 h time step was chosen which is small enough to model the main discharge variations, since the catchment response time is estimated to be between 1 and 2 days.

Forcing variables

For the two seasons considered in this study, the 6 h time step rainfields were kriged at 1 km resolution by using a climatological spherical variogram with range of 30 km and a zero nugget (Wesson and Pegram, 2006).

As no evapotranspiration data are available for the simulated periods on the catchment, the mean annual evapotranspiration over the region was used and disaggregated at a daily time step, according to a mean seasonal signal determined by McKenzie and Craig (1999).

3.2 TOPKAPI parameter adjustment

A priori estimation of the parameters

Because of its physical basis, the model parameters can be estimated a priori from the catchment characteristics (Liu and Todini, 2002). The priori values or range of values of the parameters of the model are reported in Table 3, as well as the data and/or literature references that were used to infer the values. Among the 13 parameters of the TOPKAPI model, 7 are spatially variable. As a complement to Table 3, Fig. 2b shows the maps of the spatially variable parameters and their link to the data available over the Liebenbergsvlei catchment (Fig. 2a). A Geographical Information System was used in junction with the DEM in order to (i) compute the slope ($tan(\beta)$) of each cell (ii) delineate the stream network and (iii) compute the Strahler orders of each channel reach (Strahler, 1957). The ordering method of Strahler is used to infer the values of the channel roughness Manning's coefficients n_c. In Liu and Todini (2002), channel orders of 1, 2, 3 and 4 were assigned values of 0.045, 0.04, 0.035 and 0.035 for the Upper Reno catchment in Italy. In the absence of any information about the channel reach properties, these values were assumed to be suitable as starting values for the Liebenbergsvlei catchment. The values of the overland roughness Manning's coefficient n_o were derived from the landuse/cover map (GLCC, 1997), using the tables in Chow et al. (1988). Maps of soil depths L and saturated soil moisture θ_s were already available over the catchment in the data set of soil properties (SIRI 1987). The residual soil moisture θ_s and the hydraulic conductivity at saturation K_s were derived from the soil texture map (Midgely et al., 1994) according to parameter tables for the Green-Ampt infiltration model (Maidment, 1993). As in Liu and Todini (2002), the pore-size

distribution parameter α_s was uniformly set to the value 2.5. A sensitivity analysis (not presented here) showed that varying the value of α_s in the realistic range of its values (between 2 and 4 according to Liu and Todini, 2002) had only a small influence on the simulations. As a first approximation, and because of the relatively homogeneous cropland/grassland landcover, the crop factor k_c was assumed to be spatially uniform over the catchment and equal to 1.

The other parameters concern the channel geometry. The threshold value of the area over which the water is considered to be drained in a channel ($A_{\text{threshold}}$) was fixed at 25 km^2 after checking the limit of the streams with those shown on 1:250 000 maps. The minimum and maximum width of the channel (respectively W_{min} and W_{max}) were fixed at respectively 5 m and 35 m (estimation from pictures taken at the flow station). A linear relationship between the drained area and the channel width at a point proposed by Liu and Todini (2002) was used to determine the channel width along the catchment.

Because of the uncertainty in the estimation of the catchment's characteristics from a priori datasets, a calibration was required.

Calibration procedure

The method used to calibrate the model was inspired by the Ordered Physics-based Parameter Adjustment method (OPPA) proposed by Vieux et al. (2004). This method aims to calibrate the physically distributed hydrological model parameters in a specific order. First the parameters controlling the production of the runoff are adjusted such that a discharge volume objective function is minimized. Then the parameters controlling the runoff routing are adjusted such that a discharge timing objective function is minimized. According to a sensitivity analysis of the model parameters (not shown here, but also in accordance with the work of Liu et al., 2005), the most important parameters controlling the production in TOPKAPI are the soil depth L and the soil conductivity K_s, while the timing of runoff is mainly controlled by the Manning roughness of the channel n_c and of the overland surfacen_o. In the absence of any quantitative information, the initial soil moisture V_{s_initial}, which was shown to have a strong influence on

the simulations, was also calibrated. Ten values of mean catchment saturation between 1 and 90% were tested.

In order to have realistic patterns of initial soil moisture fields that preserve the most likely spatial distribution of soil moisture on the catchment, the model was run with the a priori parameters and zero rainfall input. The initial soil saturation of the catchment was 100% (meaning that each cell was 100% saturated). At each 6 hourly simulation time step, the mean catchment saturation was calculated. From these simulations, 10 soil moisture maps were extracted corresponding as closely as possible to mean saturation levels regularly spaced between 90% and 1%. These maps were used as reference initial soil moisture maps.

As suggested by Vieux et al. (2004) and by most of the studies dealing with the calibration of distributed hydrological models, the parameters are not tuned independently for each cell, but the parameter map is calibrated by using a multiplicative factor applied uniformly in space. For our application the four multiplicative factors to be applied were fac_L (for the soil depth), fac_{Ks} (for the hydraulic conductivity), fac_{no} (for the overland roughness) and fac_{nc} (for the channel roughness).

The trio of parameters (fac_L, fac_{Ks}, $V_{s\_initial}$) and the pair of parameters (fac_{no}, fac_{nc}) were calibrated independently, after verifying that they were effectively independent, meaning that their variation influenced exclusively (respectively) the production and the timing of runoff. The triplet (fac_L, fac_{Ks}, $V_{s\_initial}$) was adjusted in order to minimize the Root Mean Square Error (RMSE) objective function comparing modelled and observed discharge volumes aggregated at a monthly time step. Then the pair (fac_{no}, fac_{nc}) was adjusted using the regression coefficient (R^2) in order to match the timing of observed and modelled discharges at a 6 h time step.

In order to reduce the computation time required by the calibration procedure, the calibration was carried out using the flows estimated at the station 2 (see Fig. 3). At this station, the drainage area is 3563 km^2, which effectively preserves the main soil heterogeneity of the entire catchment.

3.3 Results

Figure 5a shows the results of the calibration. There is a good correspondence between observed and modelled hydrographs (Nash efficiency of more than 0.8). In Table 3 the values of the four calibrated multiplying factors are reported. It is worth noting that all the values of the parameters estimated a priori were quite appropriate except for the soil conductivity which has been increased by a factor 100; (this aspect will be discussed in Sect. 5). The initial soil moisture was also adjusted by calibration to a mean value of 40% over the catchment.

As a verification of the relevance of the calibration procedure and its effect on other discharge time series, the calibrated model was applied to the entire catchment. For the same season (Season 1) the observed and modelled discharges at the outlet of the catchment (Station 1) are plotted in Fig. 5b. Globally, there is once again a good correspondence between observed and modelled flows, however at some points, the observed data seem to be unreliable since some peaks recorded at Station 2 do not appear as they should at the outlet and the recession shape of the main peak discharge seems somewhat unrealistic. In order to check the verification procedure on more reliable data, the model was then applied to an independent season (Season 2). During this season, the discharges are influenced by the inter-basin transfer flows arriving from Lesotho. In order to reliably compare the modelled and observed discharges, the external flows observed at Station 3 were injected at the location the closest to Station 3. Again in absence of any information about the initial soil moisture, the value of 40% calibrated for Season 1 was assumed to be applicable for Season 2. Results are plotted in Figs. 5c and d. Again, good simulations of the hydrographs were obtained even if the main peak discharges are slightly underestimated. One can also note that the timing of the flows is remarkable, especially at the beginning of the season, when in absence of rainfall, the flows are mainly explained by the external flows that are routed from the upper part of the catchment; these appear pulsed because of hydropower generation.

4 Comparison of remotely sensed and modelled soil moisture

4.1 Definition of a remotely sensed and modelled Soil Water Index (SWI)

As already noted in Sect. 2.2, the remotely sensed soil moisture estimation is representative of the relative water content of the first 5 centimetres of topsoil effectively 'seen' by the scatterometer. However, for the purpose of the present study, which is to compare the soil moisture as modelled by TOPKAPI and the remotely sensed soil moisture, the variable of concern is the soil moisture in the entire soil layer.

In order to provide a reliable comparison, the soil moisture in the whole soil layer must thus be obtained from the surface soil moisture estimated by the satellite. The method used here to estimate the soil moisture profile in the soil horizon was proposed by Wagner et al. (1999c). It is a simple conceptual infiltration model based on an exponential filter, temporally smoothing the signal of the (instantaneously estimated) relative surface soil moisture to give the Soil Water Index, *SWI*:

$$SWI(t) = \frac{\sum_i m_s(t)\, e^{-(t-t_i)/T}}{\sum_i e^{-(t-t_i)/T}} \quad \text{for } t_i \le t \tag{4}$$

where m_s is the surface soil moisture estimate from the ERS scatterometer defined in Eq. (1). T represents a characteristic time length depending to the soil properties (mainly soil depth, diffusivity and moisture state). To maintain the crucial independence of the physically based approach of TOPKAPI and the remotely sensed soil moisture estimates, it was decided not to refine the estimation of the parameter T for the particular study area by using the soil data. Thus the value of T=20 days, suggested by Wagner et al. (1999c) as an average value, was retained.

A surrogate for *SWI* can easily be defined for TOPKAPI by computing the soil saturation at each catchment cell, for each time step of the simulation.

Two different scales are considered to make the comparison between the modelled

and remotely sensed soil moisture. The first is the catchment scale, at this scale: (i) the mean catchment *SWI* is computed from the hydrological model by averaging over the catchment the *SWI* computed at each cell, (ii) the mean catchment *SWI* is computed from the scatterometer data, by averaging over the catchment the SWI computed for the scatterometer grid points in and surrounding the catchment (the average being weighted according to Thiessen polygons). The second scale is the scatterometer footprint scale, which is smaller than the catchment scale. This corresponds to the original scatterometer resolution defined by a circle of diameter 50 km. The footprint *SWI* is computed from the hydrological model by averaging the *SWI* computed at each cell within the footprint. In order to make a robust comparison, only the three footprints showing the largest areal coverage of the catchment were considered

4.2 Results

At catchment scale

The modelled and remotely sensed mean catchment *SWI* are compared in Figure 6 for the two modelled seasons, at the time step of ten days imposed by the ERS sampling interval. There is a very good correspondence between the two SWI estimates, as illustrated by the regression coefficients (R^2) of 0.780 for the first season and 0.922 for the second season. According to the regression equation, a slight relative bias is observed (which seems to be independent of the season) that is likely to be due to uncertainties in the estimation of the dry and wet reference backscatter values σ^0_{dry} and σ^0_{wet} used for the calculation of the remotely sensed surface soil moisture value (Eq. 1). Despite this, the order of magnitude of the remotely sensed and the modelled SWI is still very similar. As an interesting example, the value of the initial soil moisture, which has been calibrated at 40%, could have been estimated by using the remotely sensed value. This result is very encouraging since the initialization of hydrological models after a dormant period remains a constant problem in hydrology.

At footprint scale

Figures 7 and 8 show respectively the remotely sensed and the modelled SWI at footprint scale and the associated scatter plots. The results show that the good correspondence already found at catchment scale is retrieved at the smaller scale of the footprint. The correlations are still very good (greater than 0.7), while according to the regression equations, the bias between the two SWI is relatively stable and appears to be independent of season and location.

5 Discussion and conclusion

The paper aimed to compare, for the purpose of corroboration, not validation, two independent approaches used to estimate soil moisture at the scale of a region-sized catchment (Liebenbergsvlei, 4625 km^2, South Africa). The first estimation was derived from physically based hydrological modelling of the catchment using the TOPKAPI model (Liu and Todini, 2002) and the second was derived from the remotely sensed observations of the scatterometer on board on the ERS satellite.

A calibration procedure of the TOPKAPI model has been carried out consisting of the adjustment of the four most sensitive parameters of the model according to runoff production and routing. The results of the calibration showed that the values of the parameters of the TOPKAPI can be estimated a priori with a very good reliability from information about the topography and the soil properties associated to parameter tables from the literature. The exception was the hydraulic conductivity at saturation, which had to be multiplied by a factor 100 to capture the phenomenon of lateral flows in the subsurface. A very good agreement was found between observed and modelled hydrographs of the Liebenbergsvlei catchment for both calibration and verification period.

Obviously one can argue that such a multiplying factor of K_s is not physically realistic. However, one has to be aware that the values of K_s estimated a priori were derived

from Green-Ampt infiltration model tables that are associated with the local scale of a column of soil and for vertical infiltration fluxes. The alternative behavior of the horizontal hydraulic conductivity has already been reported in the literature, particularly by the developers and users of TOPMODEL (Beven and Kirkby, 1979; Beven, 1997) and is mainly attributed to the fact that the lateral fluxes controlled by the topography are, in the subsurface, likely to occur in preferential paths (macropores, root pipes, soil cracks etc.). The calibration procedure tends to show that rapid flows in preferential paths are effectively dominant in the Liebenbergsvlei catchment. Another reason might be that the production of runoff can also be due to infiltration excess mechanisms (or Hortonian processes). Such processes are indeed likely to occur especially in semi-arid areas, as in the Liebenbergsvlei catchment. The difficulty of the model to respond to observed precipitation in the beginning of the wet season is probably linked to the production of Hortonian runoff, when the soils are dried and potentially crusted and the vegetation is not fully developed. However, the assumption of the predominance of subsurface flows and the associated saturation excess runoff production seems to be realistic in the area for the major part the season. Some field experiments have been conducted at the hillslope scale in the region which tend to confirm that saturation excess production of runoff is predominant (C. Everson, 2007, personal communication). These experiments suggest that the TOPKAPI hypothesis and the calibrated hydraulic conductivity are quite realistic on the Liebenbergsvlei catchment. It is also worth noting that a part of this increase of the hydraulic conductivity could be explained by the resolution of 1 km used to implement the model. Martina (2004) identified the 1 km resolution as the upper limit of physical scale above which the TOPKAPI model parameters no longer match the physics.

The comparison between the modelled and the remotely sensed soil moisture estimates were done using the computation of the Soil Water Index (*SWI*) which is the relative soil moisture through the soil depth. As the satellite only provides soil moisture for the topsoil layer (first 5 centimeters), a conceptual infiltration model developed by Wagner et al. (1999c) was applied to the surface soil moisture estimates in order to

estimate a remotely sensed *SWI*. The comparison between the modelled and remotely sensed *SWI* was shown to be very good with regression coefficient greater than 0.7.

One can of course question the reason for such a good correspondence between the two independent soil moisture estimates. This is likely due to three main reasons:

1. The Soil Water Index is considered in the present study, meaning the relative water content along the soil depth. Many studies focus on vertical transfers (Soil Vegetation Atmosphere Transfer model) but ignore the lateral transfers (horizontal subsurface flows) that occur in the soil layer and partly control the soil moisture. In the present study, the lateral transfers are explicitly modelled by the TOPKAPI model to represent the subsurface flow processes.

2. The scatterometer estimations are very sensitive to the vegetation and are better in less vegetated regions (Wagner et al., 1999b). In the Liebenbergsvlei, the grassland and cropland surfaces are likely to result in reliable estimates of soil moisture from this source.

3. The remotely sensed *SWI* comes from a conceptual infiltration model (Wagner et al., 1999c) whose parameters seem to be quite suitable for the study area.

4. The raingauge network is characterized by a very high spatial density of well calibrated pluviometers that gives a reliable estimation of the precipitation amount at the catchment scale.

The results obtained at this stage are thus very encouraging for (i) hydrological modelling and the possibility of using remotely sensed soil moisture to validate the models and also to initialize them; assimilation of the remotely sensed soil moisture data into hydrological models during simulations is also an exciting possibility, (ii) remote sensing and the possibility of using physically based hydrological models to validate and disaggregate the soil moisture estimations down to fine spatial scales.

Further research will aim to improve the modelling of the vertical fluxes that explicitly represent the vertical water transfers in the soil and will allow direct comparison

between the remotely sensed soil moisture at the surface (first 5 centimeters of soil) without being dependant on the conceptual infiltration model used in the present study to infer the soil moisture profile from the surface remotely sensed soil moisture. Such a complete physically based model should help to better understand the processes that control the soil moisture patterns at regional scale and will be applied as a physically based soil moisture back-calculation and disaggregation tool.

Acknowledgements. This research was funded by the Water Research Commission (South Africa) and also formed part of the TIGER SHARE program initiated by the European Space Agency. Supplementary support was provided by the collaboration project between France and South Africa SAFeWater.

References

Aubert D., Loumagne C., and Oudin L.: Sequential assimilation of soil moisture and streamflow data in a conceptual rainfall-runoff model, J. Hydrol., 280, 145–161, 2003.

Beven, K.: TOPMODEL: a critique, Hydrol. Process, 11(9), 1069–1086, 1997.

Beven K. and Kirkby M.: A physically-based variable contributing area model of basin hydrology, Hydrol. Sci. Bull., 24, 43–69, 1979.

Biftu, G. F. and Gan, T. Y.: Semi-distributed, physically based, hydrologic modeling of thePaddle River Basin, Alberta, using remotely sensed data, J. Hydrol., 244, 137–156, 2001.

Blyth, E.: Modelling soil moisture for a grassland and a woodland site in south-east England, Hydrol. Earth Syst. Sci., 6(1), 39–47, 2002.

Brooks, R. H. and Corey, A. T.: Hydraulic properties of porous media. Hydrology papers, No. 3. Colorado State University, Colorado, 1964.

Bruckler, L. and Witono, H.: Use of remotely sensed soil moisture content as boundary conditions in soil-atmosphere water transport modeling. 2. Estimating soil water balance, Water Resour. Res., 25, 2437–2447, 1989.

Chow, V. T., Maidment, D. R., and Mays, L. R.: Applied Hydrology, McGraw-Hill, New York.,1988.

De Lannoy, G. J. M., Verhoest, N. E. C., Houser, P. R., Gish, T. J., Meirvenne, M.: Spatial and

temporal characteristics of soil moisture in an intensively monitored agricultural field (OPE3), J. Hydrol., 331, 719–730, 2006.
DLSI: A digital elevation model for South Africa. Directorate of Land Surveys And Information. South Africa, 1996.
Dunne, T.: Field studies of hillslope flow process. Hillslope Hydrology, edited by: Kirkby, M. J., 227–293. Wiley, New York, 1978.
Entekhabi, D., Rodriguez-Iturbe, I., and Castelli, F.: Mutual interaction of soil moisture state and atmospheric processes, J. Hydrol., 184, 3–17, 1996.
Gerald, C. F. and Wheatley, P. O.: Applied numerical analysis. Fourth Edition, Addison-Wesley, 1992.
GLCC: Global Land Cover Characteristics. United States Geological Survey (USGS), http://edcdaac.usgs.gov/glcc, 1997.
Grayson, R. B, Western, A. W., and Chiew, F. H. S.: Preferred states in spatial soil moisture patterns: Local and nonlocal controls, Water Resour. Res., 33(12), 2897–2908, 1997.
Hébrard, O., Voltz, M., Andrieux, P., and Moussa, R.: Spatio-temporal distribution of soil surface moisture in a heterogeneously farmed Mediterranean catchment, J. Hydrol., 329, 110–121, 2006.
Hodnett, M. G. and Bell, J. P.: Soil moisture investigations of groundwater recharge through black cotton soils in Madhya Pradesh, India, Hydrol. Sci. J., 31(3), 361–381, 1986.
Houser, P. R., Shuttleworth, W. J., Famiglietti, J. S., Gupta, H. V., Syed, K. H., and Goodrich, D. C.: Integration of soil moisture remote sensing and hydrologic modeling using data assimilation, Water Resour. Res., 34(12), 3405–3420, 1998.
Kostov, K. G. and Jackson, T. J.: Estimating profile soil moisture from surface layer measurements– a review. Proceedings of the international Society for Optical Engineering (SPIE), Orlando, 11–14 April, 125–136, 1993.
Liu, Z. and Todini, E.: Towards a comprehensive physically-based rainfall-runoff model, Hydrol. Earth Syst. Sci., 6(5), 859–881, 2002.
Liu, Z., Mario, L. V., and Todini, E.: Flood forecasting using a fully distributed model: application of the TOPKAPI model to the Upper Xixian catchment, Hydrol. Earth Syst. Sci., 9, 347–364, 2005, http://www.hydrol-earth-syst-sci.net/9/347/2005/.
Martina, M. L. V.: The distributed physically based modelling of the rainfall-runoff process, PhD Thesis. University of Bologna, 2004.

McKenzie, R. S. and Craig, A. R.: Evaporation losses from South African rivers. WRC report; no.638/1/99. Pretoria: Water Research Commission (South Africa), 1999.
McNamara, J. P., Chandler, D., Seyfried, M., and Achet, S.: Soil moisture states, lateral flow, and streamflow generation in a semi-arid, snowmelt-driven catchment, Hydrol. Process., 19, 4023–4038, 2005.
Merz, B. and Plate, E. J.: An analysis of the effect of spatial variability of soil and soil moisture on runoff, Water Resour. Res., 33, 2909–2922, 1997.
Midgley, D. C., Pitman, W. V., and Middleton, B. J.: Surface water resources of South Africa 1990. Water Research Comission Report NO 298/2.2/94, 1994.
Ottlé, C. and Vidal-Madjar, D.: Assimilation of soil moisture inferred from infrared remote sensing in a hydrological model over the HAPEX-MOBILHY region, J. Hydrol., 158(3–4), 241–264, 1994.
Parajka, J., Naeimi, V., Blöschl, G., Wagner, W., Merz, R., and Scipal, K.: Assimilating scatterometer soil moisture data into conceptual hydrological models at the regional scale, Hydrol. Earth Syst. Sci., 10, 353–368, 2006, http://www.hydrol-earth-syst-sci.net/10/353/2006/.
Pauwels, V. R. N., Hoeben, R., Verhoest, N. E. C., De Troch, F. P., and De Troch, P. A.: Improvement of TOPLATS-based discharge predictions through assimilation of ERS-based remotely sensed soil moisture values, Hydrol. Process, 16, 995–1013, 2002.
Pellenq, J., Kalma, J., Boulet, G., Saulnier, G.-M., Wooldridge, S., Kerr, Y., and Chehbouni, A.: A disaggregation scheme for soil moisture based topography and soil depth, J. Hydrol., 276, 112–127, 2003.
Reichle, R. H., Mc Laughlin, D. B., and Entekhabi, D.: Variationnal data assimilation of microwave radiobrightness observations for land surface hydrology applications, IEEE Trans. Geosci. Remote Sensing, 39(8), 1708–1718, 2001.
Rodriguez-Iturbe, I.: Ecohydrology: a hydrologic perspective of climate-soil-vegetation dynamics,Water Resour. Res., 36, 3–9, 2000.
SIRI: Land Type Series. Department of Agriculture and Water Supply, Soil and Irrigation Research Institute. Memoirs on the Agricultural Natural Resources of South Africa. Pretoria, 1987.
Strahler, A. N.: Quantitative analysis of watershed geomorphology, Trans. Amer. Geophys. Union, 38, 913–920, 1957.
Vieux, B. E., Cui, Z., and Gaur, A.: Evaluation of a physics-based distributed hydrologic model

for flood forecasting, J. Hydrol., 298, 155–177, 2004.
Wagner, W., Noll, G., Borgeaud, M., and Rott, H.: Monitoring soil moisture over the Canadian prairies with ERS scatterometer, IEEE Trans. Geosci. Remote Sens., 37(1), 200–216, 1999a.
Wagner, W., Lemoine, G., Borgeaud, M., and Rott, H.: A study of vegetation cover effects on ERS scatterometer data, IEEE Trans. Geosci. Remote Sens., 37(2), 938–948, 1999b.
Wagner, W., Lemoine, G., and Rott, H.: A method for estimating soil moisture from ERS scatterometer and soil data, Remote Sens. Environ., 70, 191–207, 1999c.
Wagner, W., Scipal, K., Pathe, C., Gerten, D., Lucht,W., and Rudolf, B.: Evaluation of the agreement between the first global remotely sensed soil moisture data with model and precipitation data, J. Geophys. Res. Atmos., 108(D19), 4611, doi:10.1029/2003JD003663, 2003.
Wagner, W., Blöschl, G., Pampaloni, P., Calvet, J.-C., Bizzarri, B., Wigneron, J.-P., and Kerr, Y.: Operational readiness of microwave remote sensing of soil moisture for hydrologic applications, Nordic Hydrology, 38(1), 1–20, 2007.
Walker, J. P., Willgoose, G. R., and Kalma, J. D.: One-dimensional soil moisture profile retrieval by assimilation of near-surface observations: a comparison of retrieval algorithms, Adv. Water Resour., 24, 631–650, 2001.
Wesson, S. M. and Pegram, G. G. S.: Improved radar rainfall estimation at ground level, Nat.Hazards Earth Syst. Sci., 6(3), 323–342, 2006.
Western, A. W. and Blöschl, G.: On the spatial scaling of soil moisture, J. Hydrol., 217, 203–224, 1999.
Western, A. W., Grayson, R. B., and Blöschl, G.: Scaling of soil moisture: a hydrologic perspective, Ann. Rev. Earth Planet. Sci., 30, 149–180, 2002.

Table 1. Expressions and/or typical values of the coefficient b_i and α of Eq. (3) for each component store in a cell.

Reservoir	b_i	α
Soil	$b_i = \frac{C_{s_i} X}{X^{2\alpha}}$ with $C_{s_i} = \frac{L_i K_{s_i} \tan(\beta_i)}{(\theta_{s_i} - \theta_{r_i})^{\alpha} L_i^{\alpha}}$ where: -L_i is the soil depth -K_{s_i} is the saturated hydraulic conductivity –tan (β_i) is the tangent of the ground slope β_i -θ_{s_i} is the saturated soil moisture content -θ_{r_i} is the residual soil moisture content	$\alpha = \alpha_s$ with $2 \leq \alpha_s \leq 4$ Where α_s is a pore-size distribution parameter (Brooks and Corey, 1964)
Overland	$b_i = \frac{C_{o_i} X}{X^{2\alpha}}$ with $C_{o_i} = \frac{1}{n_{o_i}} \sqrt{\tan(\beta_i)}$ -n_{o_i} is Manning's roughness coefficient -tan (β_i) is the tangent of the ground slope β_i	$\alpha = \alpha_o = 5/3$
Channel	$b_i = \frac{C_{c_i} W_i}{(X W_i)^{\alpha}}$ with $C_{c_i} = \frac{1}{n_{c_i}} \sqrt{\tan(\beta_i)}$ - W_i is the width of the channel -n_{c_i} is Manning's roughness coefficient -tan (β_i) is the tangent of the ground slope β_i	$\alpha = \alpha_c = 5/3$

Table 2. Variables computed at each cell i between time t and Δt: see Fig. 4 for flow paths.

	Initial value: Volume at t	Inflow rates during $[t, t+\Delta t]$	*ODE solution:* Volume at $t+\Delta t$	Outflow rates during $[t, t+\Delta t]$	*Flow partitioning:* Flow rate to next cell during $[t, t+\Delta t]$
Soil	$V_{s_i}(t)$	$Q_{s_i}^{\text{in}} = P_i X^2 + Q_{s_i}^{\text{up}} + Q_{o_i}^{\text{up}}$	$V_{s_i}(t+\Delta t)$	$Q_{s_i}^{\text{out}} = Q_{s_i}^{\text{in}} - \frac{V_{s_i}(t+\Delta t) - V_{s_i}(t)}{\Delta t}$	*To next soil reservoir* $Q_{s_i}^{\text{out}} - Q_{s_i}^{\text{excess}} - \frac{W_i}{X} Q_{s_i}^{\text{out}}$
Overland	$V_{o_i}(t)$	$Q_{o_i}^{\text{in}} = Q_{s_i}^{\text{excess}} = \max\left(0, Q_{s_i}^{\text{out}} - Q_{s\max i}\right)$ with $Q_{s\max_i} = X K_{s_i} L_i \tan(\beta_i)$	$V_{o_i}(t+\Delta t)$	$Q_{o_i}^{\text{out}} = Q_{o_i}^{\text{in}} - \frac{V_{o_i}(t+\Delta t) - V_{o_i}(t)}{\Delta t}$	*To next soil reservoir* $Q_{o_i}^{\text{out}} - \frac{W_i}{X} Q_{o_i}^{\text{out}}$
Channel	$V_{c_i}(t)$	$Q_{c_i}^{\text{in}} = Q_{c_i}^{\text{up}} + \frac{W_i}{X} Q_{s_i}^{\text{out}} + \frac{W_i}{X} Q_{o_i}^{\text{out}}$	$V_{c_i}(t+\Delta t)$	$Q_{c_i}^{\text{out}} = Q_{c_i}^{\text{in}} - \frac{V_{c_i}(t+\Delta t) - V_{c_i}(t)}{\Delta t}$	*To next channel* $Q_{c_i}^{\text{out}}$

Table 3. Values of the TOPKAPI model parameters estimated a priori from data and literature, and values of multiplying factors used for the calibration procedure.

Parameter		Value *a priori*	Origin and references	Calibrated multiplying factor value	
Spatially variable (cf. Figure 2b)					
Surface Slope	$tan\,\beta$	1.7E-4–1.81E-1	DEM (DLSI,1996)		
Depth of surface soil layer (m)	L	0.33–0.81	Soil type map (SIRI,1987)	fac_L	1.1
Saturated hydraulic conductivity ($m.s^{-1}$)	K_s	1.67E-6–5.18E-4	Soil texture map (Midgley et al., 1994) + Maidment (1993)	fac_{Ks}	100.
Residual soil moisture content	θ_r	0.02–0.09	Soil texture map (Midgley et al., 1994) + Maidment (1993)		
Saturated soil moisture content	θ_s	0.41–0.44	Soil type map (SIRI,1987)		
Manning's surface roughness coeff.	n_o	0.025–0.1	Landuse map (GLCC, 1997) + Chow et al. (1988)	fac_{no}	1.
Manning's channel roughness coeff.	n_c	0.035–0.045	Strahler order method (Liu and Todini 2002)	fac_{nc}	1.7
Constant					
Horizontal dimension of cell (m)	X	1000	DEM (DLSI,1996)		
Non-linear soil exponent	α_s	2.5	Liu and Todini (2002)		
Max. channel width at outlet (m)	W_{max}	35	Field pictures		
Min. channel width for $A_{threshold}$ (m)	W_{min}	5	-		
Area required to initiate channel (m^2)	$A_{threshold}$	2500000	-		
Crop factor	k_c	1.	Landuse map (GLCC, 1997)		

HESSD
4, 2273–2306, 2007

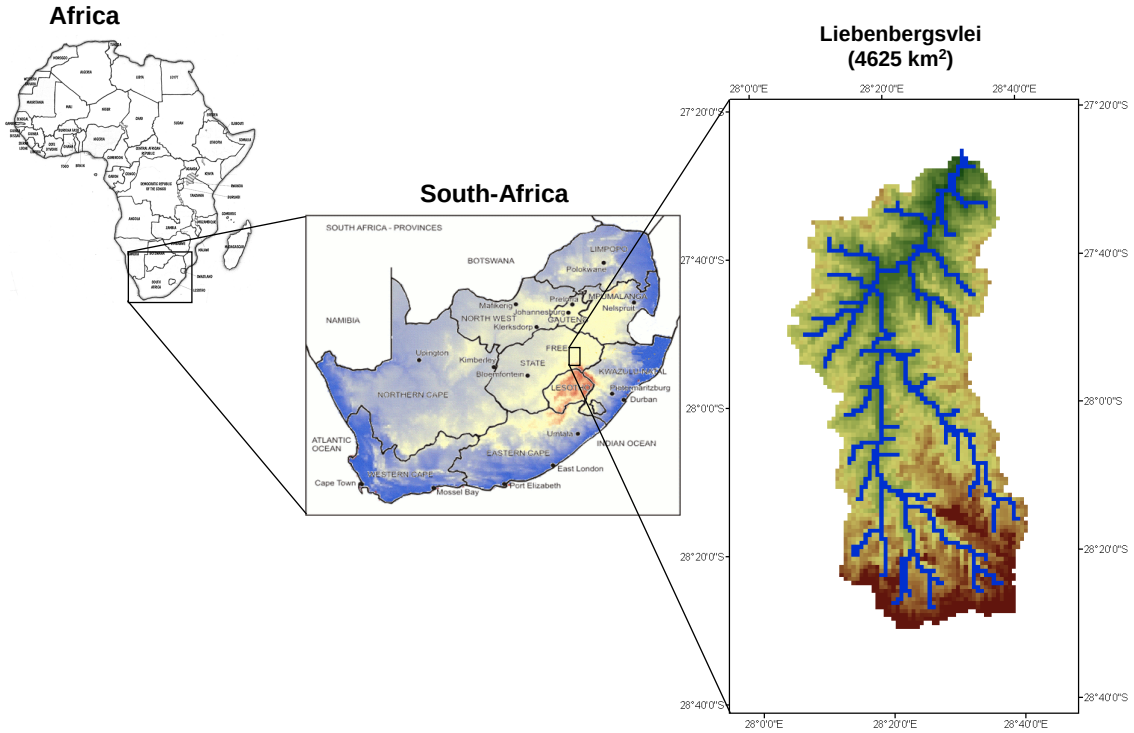

Fig. 1. The Liebenbergsvlei catchment (4625 km^2) in South Africa.

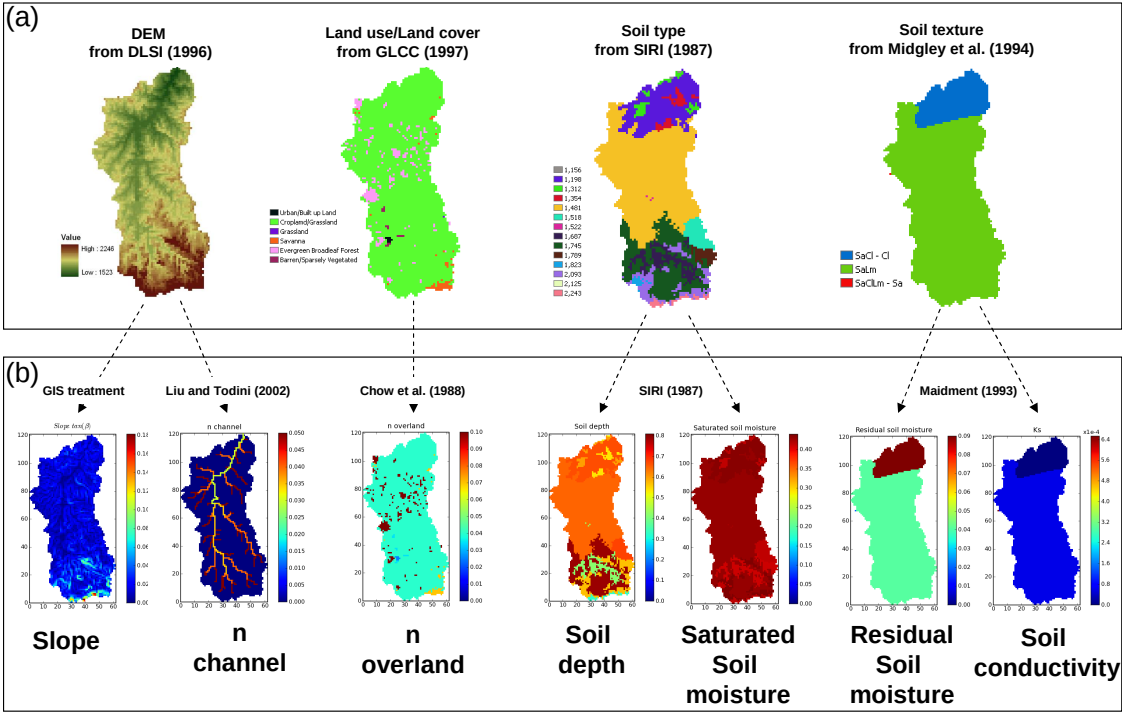

Fig. 2. (a) Catchment characteristics. **(b)** Estimations a priori of the TOPKAPI model parameters.

HESSD
4, 2273–2306, 2007

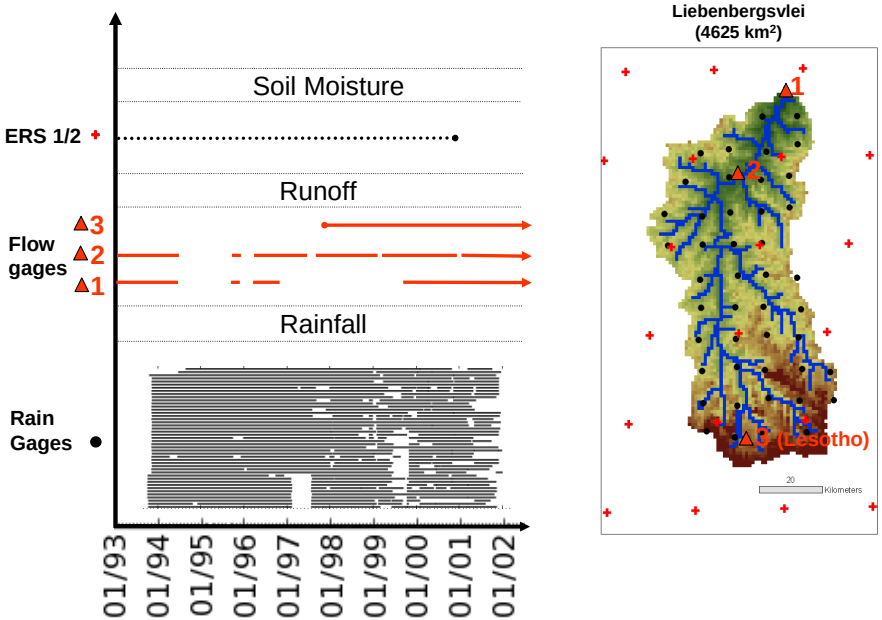

Fig. 3. Hydrological data availability on the Liebenbergsvlei catchment, South Africa.

HESSD
4, 2273–2306, 2007

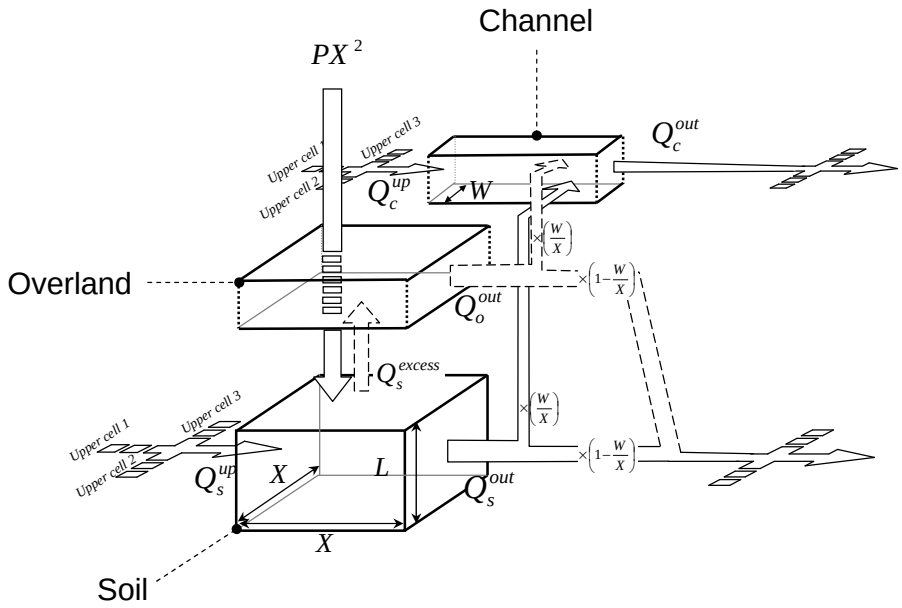

Fig. 4. Water balance in the TOPKAPI model (note that for clarity, the evapotranspiration losses are not represented on the figure).

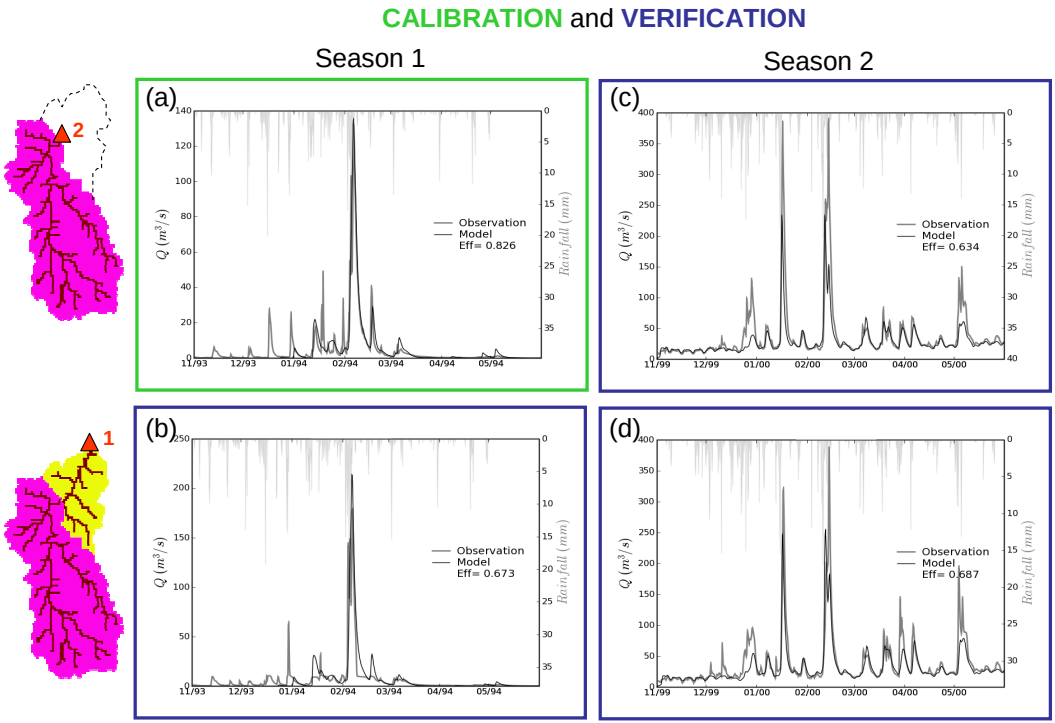

Fig. 5. Modelled and observed hydrographs. Calibration **(a)** and verification (**b**, **c**, **d**) of the model at two station and for two distinct 8 month seasons.

HESSD
4, 2273–2306, 2007

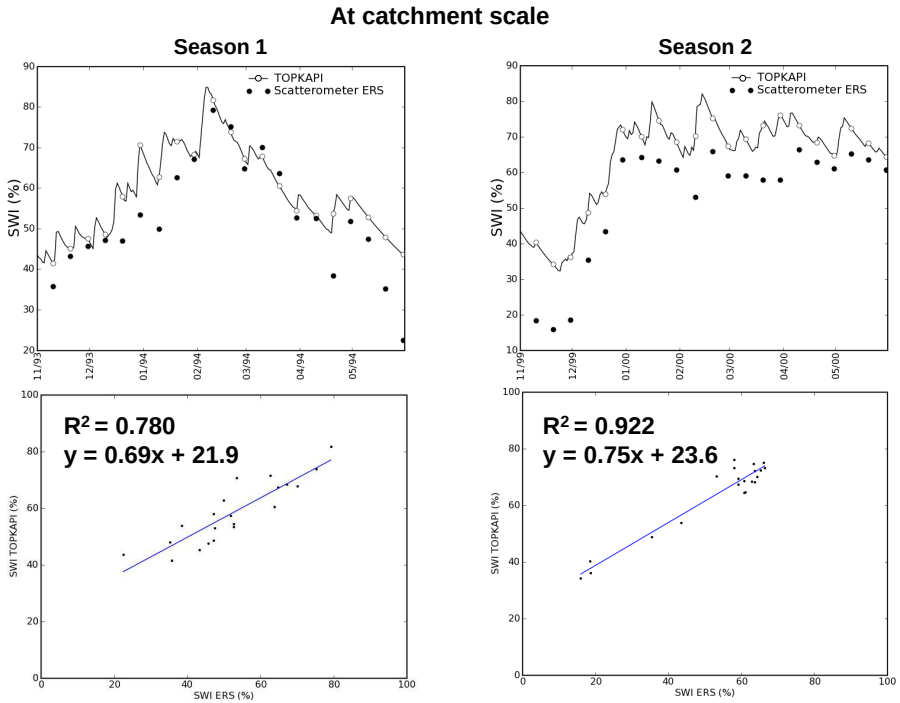

Fig. 6. Comparison between the modelled and the remotely sensed SWI computed at catchment scale. The white dots are the TOPKAPI estimates at time corresponding to the scatterometer estimates (black dots).

HESSD
4, 2273–2306, 2007

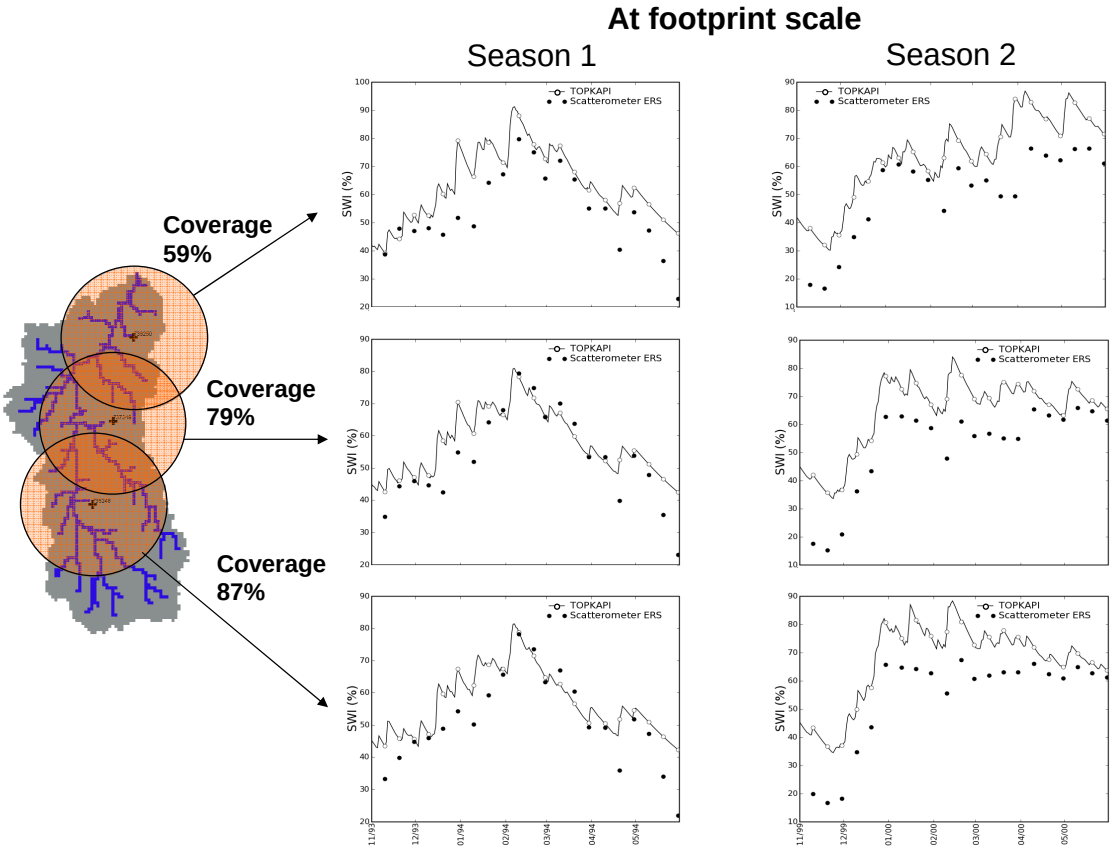

Fig. 7. Comparison of the modelled and remotely sensed Soil Water Index (SWI) at the scatterometer footprint scale.

HESSD
4, 2273–2306, 2007

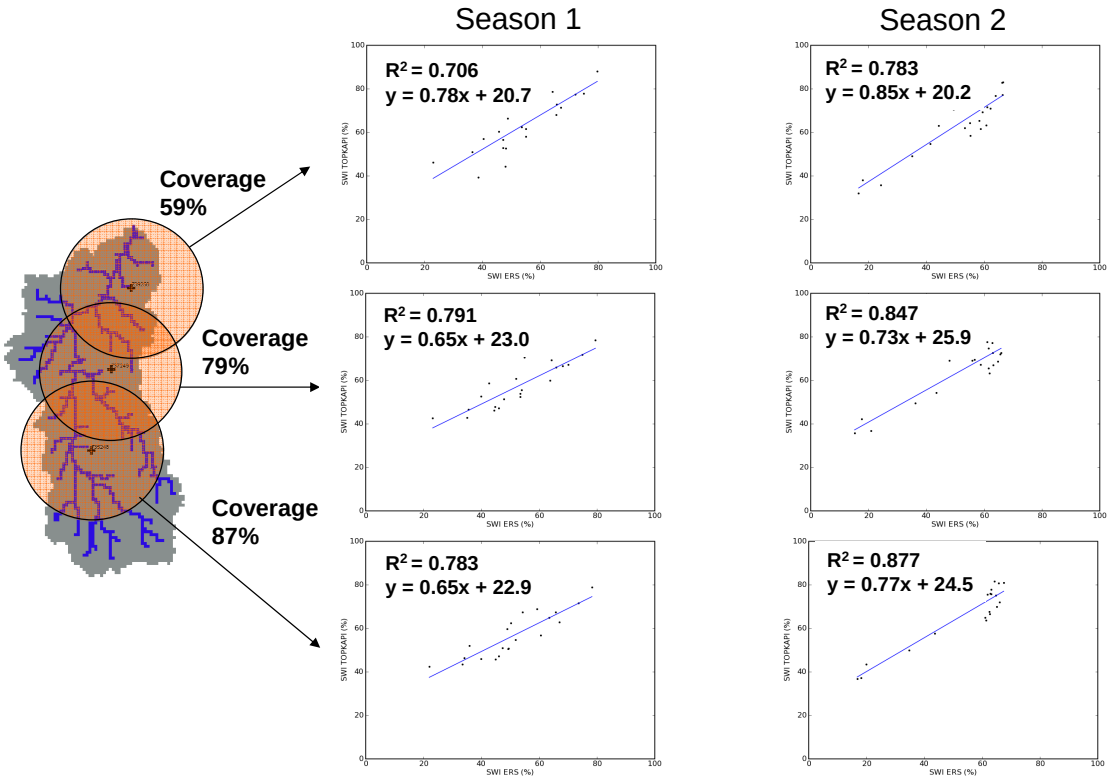

Fig. 8. Comparison of the modelled and remotely sensed Soil Water Index (SWI) at the scatterometer footprint scale (Scatter plots and regression equations).

HESSD
4, 2273–2306, 2007